JOURNAL OF CHEMICAL & ENGINEERING DATA

ARTICLE

pubs.acs.org/jced

Thermodynamics and Kinetics of Au(III) Adsorption on Silica Gel Chemically Modified by Diethylenetriamine Bis(methylene phosphonic acid)

Ping Yin,* Chunhua Wang, Yingxia Yang, Yuan Tian, and Zhongxi Yu

School of Chemistry and Materials Science, Ludong University, Yantai 264025, P. R. China

ABSTRACT: Silica gel chemically modified by diethylenetriamine bis(methylene phosphonic acid) (denoted as SG-D-P) has been developed. A thermodynamics and kinetics investigation of SG-D-P for the adsorption of Au(III) from aqueous solutions is reported in this work. The Langmuir and Freundlich isotherm models were applied to analyze the experimental data, and the best interpretation for the experimental data was given by the Langmuir isotherm equation; the maximum adsorption capacity for Au(III) is 416.67 $mg \cdot g^{-1}$ at 35 °C. The research results show that SG-D-P could reach the saturation adsorption capacity within 4 h, and its excellent adsorption capacity for Au(III) was 499.22 $mg \cdot g^{-1}$ when the initial solution concentration was 2.0 $mmol \cdot L^{-1}$ at 35 °C. Its adsorption kinetics can be modeled by a pseudo second-order rate equation, and the thermodynamic parameters ΔG, ΔH, and ΔS are -21.18 $kJ \cdot mol^{-1}$, 16.59 $kJ \cdot mol^{-1}$, and 122.86 $J \cdot K^{-1} \cdot mol^{-1}$, respectively.

1. INTRODUCTION

Hybrid materials have been of significant interest recently because their different moieties work together to give the hybrid unique properties. Among the hybrid materials, inorganic–organic hybrids offer very interesting actual and potential applications and may have prominent properties in areas such as adsorbents.[1] Because of its excellent thermal and mechanical stability, unique large surface area, and well-modified surface properties, silica gel has been widely used as an inorganic solid matrix in inorganic–organic composite materials.[2] As an amorphous inorganic polymer, silica gel is composed of internal siloxane groups (Si–O–Si) with silanol groups (Si–OH) distributed on the surface. Thus, the kinds of hybrid materials based on silica have received a great deal of attention recently because of their excellent performance in the field of chromatography, adsorption, catalysis, and so on.[3,4] The chemical modification of the skeleton of silica gel via the covalent coupling of an organic moiety is a promising approach to obtain hybrid silica gel-based materials;[5] therefore, many chemically modified silica gels have been synthesized during the past three decades. It has been found that the behavior of these solids when used as adsorbents is mainly dependent on the presence of active donor atoms such as O, S, and N of the incorporated organic moieties.[6−9]

Gold is one of the precious metals used as a global currency, and the demand for gold has shown an increasing trend because of its increasing uses in industry. Therefore, wastewater containing gold has earned great concern because of the reasons mentioned above and the increasing application of gold. Many treatment processes, such as chemical precipitation, electrodialysis, reverse osmosis, ion exchange, and adsorption, are currently used. Among these methods, adsorption is highly effective and economical and is a promising and widely applied method.[10] Therefore, effective adsorbents with strong affinities and a high loading capacity for the targeted precious metal ions have been subsequently studied. In previous work in our group, we have introduced polyamine to the surface of silica gel through the amido bond to obtain some novel adsorbents.[11] The objective of the present work was to explore a novel adsorbent containing both N donor atoms and O donor atoms in extension of our earlier work and study its thermodynamics, isotherm, and kinetics for Au(III) adsorption from aqueous solutions.

2. EXPERIMENTAL DETAILS

2.1. Materials and Methods. Silica gel (SG) of chromatographic grade [120 to 200 mesh size (0.125 to 0.074 mm)] was obtained from the Yantai Chemical Institute, Shandong Province of China. The organic solvent toluene was redistilled just before use. The silylant agent 3-chloropropyltrimethoxysilane (Jianghan Chemicals Factory, Jinzhou, China), diethylenetriamine (DETA) (Shanghai Chemical Factory of China), and the other reagents were of analytical grade and used without any further purification. Stock solutions of Au(III) were prepared by dissolving $HAuCl_4 \cdot 4H_2O$ (Sinopharm Chemical Reagent Co., Ltd., China) in distilled water, and the pH of solution was adjusted with hydrochloric acid aqueous solution (1 $mol \cdot L^{-1}$) and sodium hydroxide aqueous solution (1 $mol \cdot L^{-1}$). Distilled water was used to prepare all of the solutions.

Fourier transform infrared spectra (FTIR) of samples were reported in the range of (4000 to 400) cm^{-1} with a resolution of 4 cm^{-1}, by accumulating 32 scans using a Nicolet MAGNA-IR 550 (series II) spectrophotometer. KBr pellets were used for solid samples. The concentration of Au(III) ions was determined using a 932 model atomic absorption spectrophotometer (GBC-932A, made in Australia), equipped with an air–acetylene flame.

Received: August 8, 2010
Accepted: January 3, 2011
Published: January 21, 2011

dx.doi.org/10.1021/je100817k | *J. Chem. Eng. Data* 2011, 56, 450–457

Scheme 1. Synthesis of the Adsorbent SG-D-P

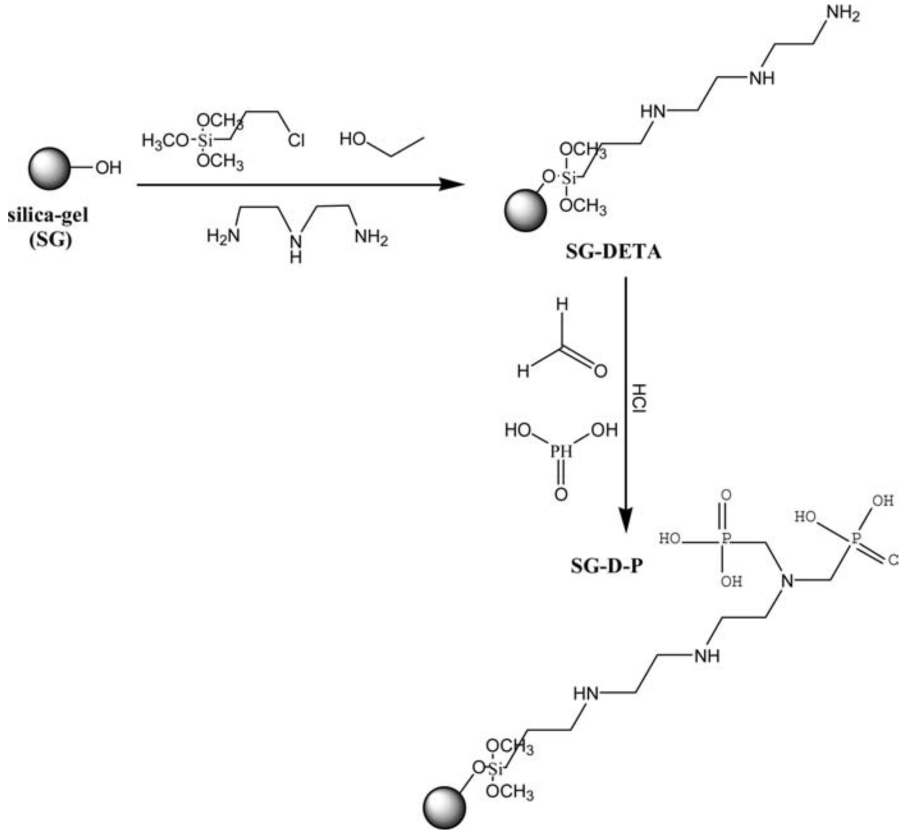

2.2. Synthesis of Silica Gel Chemically Modified Adsorbent SG-D-P. The silica gels were activated with nitric acid aqueous solution (HNO_3/H_2O = 1:1) at the refluxing temperature of 112 °C for 3 h, then dipped in hydrochloric acid aqueous solution (HCl/H_2O = 1:1) at room temperature for 6 h, and finally washed with distilled water until acid-free and dried in a muffle furnace at 160 °C for 12 h. Silica gel functionalized with amino-terminated polymers (SG→SG-DETA) was prepared according to our previous work,[11] and a summary of the procedure is as follows.

A mixture of 3-chloropropyltrimethoxysilane (10 mL) and DETA (47 mL) in ethanol (100 mL) was refluxed for 48 h with continuous stirring under a nitrogen atmosphere. After cooling, the solvent was evaporated, and then 8.0 g of activated silica gel and 120 mL of dry toluene were added. After refluxing for 12 h under a dry nitrogen atmosphere, the solids were filtered and washed with toluene and ethanol for 12 h, respectively. Finally, they were dried under vacuum over 48 h at 50 °C, and the product is referred to as SG-DETA.

A portion of 8.0 g of SG-DETA was added to 70 mL of ethanol at room temperature for 12 h; then 2.7 g of paragormaldehyde, 7.3 g of phosphorous acid, and 2.5 mL of hydrochloric acid were added. After refluxing at 90 °C for 12 h, the product (SG-D-P) was filtered off, then washed thoroughly with distilled water until it became acid-free, and finally dried under vacuum over 48 h at 50 °C. It is referred to as SG-D-P.

2.3. Computational Details. Theoretical calculations of the modified organic group have been performed with the Gaussian 03 program[12] using the B3LYP/6-31G** basis set to obtain the optimized molecular structure and vibrational wavenumbers. The frequencies for the required structure were evaluated at the B3LYP/6-31G** level to ascertain the nature of stationary points, and harmonic vibrational wavenumbers were calculated using the analytical second derivatives to confirm the convergence to a minimum of the potential surface. Moreover, Mulliken atomic charges of the modified organic group were also obtained at the B3LYP/6-31G** level.

2.4. Adsorption Experiments. Batch adsorption experiments were carried out by shaking 0.02 g of the adsorbent SG-D-P with 10 mL of metal ion solution in a series of flasks at pH 2.0 and (5 to 35) °C. At different time intervals, the adsorbent was filtrated, and the concentrations of Au(III) in solution were determined using an atomic adsorption spectrophotometer (GBC-932A).

The adsorption amount was calculated according to eq 1:

$$q = \frac{(C_o - C_e)V}{W} \qquad (1)$$

where q is the adsorption amount (mmol·g^{-1}); C_o and C_e are the initial and equilibrium concentrations of metal ion (mmol·mL^{-1}) in solution, respectively; V is the volume of the solution (mL); W is the weight of SG-D-P (g).

3. RESULTS AND DISCUSSION

The synthesis route of SG-D-P included the steps of activation of silica gel and syntheses of SG-DETA and the final product SG-D-P (Scheme 1). The introduction of the organic groups onto the hybrid material can make this material form stable chelating compounds with many transition metal ions. The aim of chemical

Scheme 2. Optimized Geometry of the Modified Organic Group

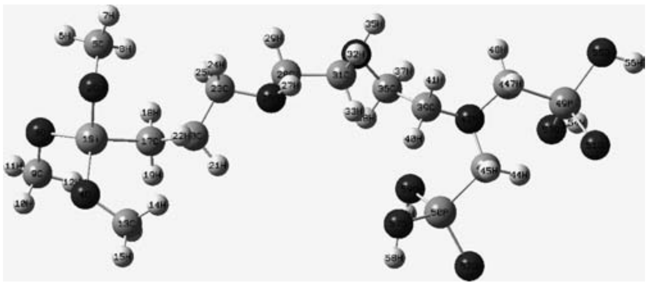

modification with amino phosphonic acid, which has both N donor atoms and O donor atoms, is to make the material have excellent coordination properties with metal ions and to obtain a novel adsorbent with a high loading capacity for metal ions. The FTIR analysis is a very useful technology in identifying the immobilization process by comparing the precursor and modified surfaces. The infrared spectra of silica gel, SG-DETA, and SG-D-P displayed important differences. In the spectrum of SG-DETA, two new bands appeared at (2933 and 2851) cm^{-1} that correspond to the typical asymmetric and symmetric stretching vibration of $-CH_2-$, due to the presence of the carbon chain of 3-chloropropyltrimethoxysilane and polyamines attached to the silica gel. A new band appeared at 1391 cm^{-1} that was assigned to the bending vibration of N−H which transferred to lower frequencies, due to the stretching vibration of the remaining Si−O of the silica gel which strongly absorbed at 1633 cm^{-1}.[7] The band around 968 cm^{-1} of the free silanol groups disappeared, due to the reaction with the alkoxide groups of the silylant agent functionalized with polyamines, and the stretching vibration of N−H overlapped in the range of (3725 to 3052) cm^{-1}. As to SG-D-P, the band at 1391 cm^{-1} ascribed to the $-NH_2$ and $-NH-$ bending vibration and the strong peak centered at 3432 cm^{-1} containing the stretching vibration of N−H were both weakened, suggesting that the phosphonic acid was successfully introduced onto the amino-terminated chelating resin silica gel. The bonds P═O at 1175 cm^{-1} and the characteristic sorption peak of P−OH around 930 cm^{-1} overlapped in the broad band between (1341 and 870) cm^{-1}.

To design the title hybrid material, we theoretically calculated the modified organic group at the B3LYP/6-31G** level in advance. In Scheme 2, the optimized structure of the modified organic group is displayed. The corresponding bond lengths and bond angles are presented in Table 1. The P49−O51 and P50−O52 bond lengths are 1.5019 Å and 1.4873 Å, respectively, which agrees with well with those values of phosphonic acid in ref 13 and is slightly longer than the experimental value (1.47 Å). Moreover, the P49−O53, P49−O55, P50−O57, and P50−O59 bond lengths are in the range (1.6139 to 1.6297) Å, comparable to those in phosphonic acid, (1.59 to 1.63) Å.[13] Table 2 presents the Mulliken atomic charges of the modified organic phosphonic acid group and shows that the oxygen atoms in phosphonic acid groups have more negative charges, and the Mulliken electronic populations of O51, O52, O53, O55, O57, and O59 were −0.784, −0.672, −0.822, −0.832, −0.916, and −1.012, respectively, which made these oxygen atoms chelate with metal ions more easily. Therefore, the designed organic groups may provide a good adsorbent for use in adsorbing metal ions from aqueous solutions.

Table 1. Optimized Geometrical Parameters Obtained at the B3LYP/6-31G** Level; the Atom Labels Are According to Scheme 2

bond length/Å	bond angle/deg	dihedral angle/deg
Si1−O2 1.6543	A(2, 1, 3) 104.4	D(3, 1, 2, 5) −38.5
Si1−C17 1.8768	A(2, 1, 4) 107.2	D(1, 2, 5, 6) 48.8
O2−C5 1.4232	A(2, 1, 17) 115.6	D(1, 3, 9, 10) 55.8
C17−C20 1.5447	A(3, 1, 4) 112.5	D(1, 4, 13, 14) 61.9
C20−C23 1.5312	A(3, 1, 17) 110.9	D(1, 17, 20, 21) 172.3
C23−N26 1.4654	A(4, 1, 17) 106.3	D(17, 20, 23, 24) 59.4
N26−C28 1.4608	A(1, 17, 20) 117.7	D(20, 23, 26, 27) −57.2
C28−C31 1.5301	A(17, 20, 23) 113.9	D(23, 26, 28, 29) 60.2
C31−N34 1.4625	A(20, 23, 26) 111.1	D(26, 28, 31, 32) −53.0
N34−C36 1.4588	A(23, 26, 28) 113.4	D(28, 31, 34, 35) 65.3
C36−C39 1.5434	A(26, 28, 31) 111.1	D(31, 34, 36, 37) 172.8
C39−N42 1.4685	A(28, 31, 34) 110.4	D(34, 36, 39, 40) 63.6
N42−C43 1.4617	A(31, 34, 36) 116.4	D(36, 39, 42, 43) −144.8
N42−C46 1.4563	A(34, 36, 39) 115.6	D(39, 42, 43, 44) −140.2
C43−P50 1.8450	A(36, 39, 42) 112.8	D(42, 43, 50, 52) −177.4
C46−P49 1.8347	A(39, 42, 43) 115.7	D(42, 43, 50, 57) −51.9
P49−O51 1.5019	A(39, 42, 46) 115.2	D(42, 43, 50, 59) 52.5
P49−O53 1.6154	A(42, 43, 50) 113.2	D(44, 43, 50, 52) 60.6
P49−O55 1.6139	A(42, 46, 49) 109.4	D(44, 43, 50, 57) −173.8
P50−O52 1.4873	A(46, 49, 51) 114.8	D(44, 43, 50, 59) −69.4
P50−O57 1.6297	A(46, 49, 53) 105.8	D(45, 43, 50, 52) −52.9
P50−O59 1.6254	A(46, 49, 55) 102.7	D(45, 43, 50, 57) 72.6
O53−H54 0.9805	A(51, 49, 53) 113.6	D(45, 43, 50, 59) 177.0
O55−H56 0.9731	A(51, 49, 55) 115.4	D(42, 46, 49, 51) −69.0
O57−H58 0.9724	A(53, 49, 55) 103.2	D(42, 46, 49, 53) 57.1
O59−H60 0.9908	A(43, 50, 52) 114.3	D(42, 46, 49, 55) 164.9
	A(43, 50, 57) 104.0	D(47, 46, 49, 51) 56.1
	A(43, 50, 59) 105.1	D(47, 46, 49, 53) −177.8
	A(52, 50, 57) 114.4	D(47, 46, 49, 55) −67.0
	A(52, 50, 59) 117.3	D(48, 46, 49, 51) 172.2
	A(57, 50, 59) 99.8	D(48, 46, 49, 53) −61.7
	A(49, 53, 54) 110.1	D(48, 46, 49, 55) 46.1
	A(49, 55, 56) 112.9	D(46, 49, 53, 54) −81.0
	A(50, 57, 58) 110.1	D(51, 49, 53, 54) 45.8
	A(50, 59, 60) 112.3	D(55, 49, 53, 54) 171.5
		D(46, 49, 55, 56) 158.7
		D(51, 49, 55, 56) 33.0
		D(53, 49, 55, 56) −91.4
		D(43, 50, 57, 58) −136.1
		D(52, 50, 57, 58) −10.7
		D(59, 50, 57, 58) 115.5
		D(43, 50, 59, 60) 54.6
		D(52, 50, 59, 60) −73.6
		D(57, 50, 59, 60) 162.2

To investigate the adsorption capacity, a wide range of concentrations of Au(III) solutions were shaken for 12 h at different temperatures. The adsorption isotherm was studied using the relationship between equilibrium adsorption capacity and equilibrium concentration at a certain temperature. The isotherm for the sorption of Au(III) onto SG-D-P at pH 2.0 and (5 to 35) °C is shown in Figure 1. It can be seen from Figure 1 that the adsorption capacities of the adsorbent increase

Table 2. Mulliken Atomic Charges of the Modified Organic Group at the B3LYP/6-31G**; the Atom Labels Are According to Scheme 2

atoms	charges	atoms	charges
Si1	1.967	O51	−0.784
O2	−0.663	O52	−0.672
O3	−0.667	O53	−0.822
O4	−0.642	H54	0.573
N26	−0.450	O55	−0.832
N34	−0.472	H56	0.521
N42	−0.056	O57	−0.916
P49	1.736	H58	0.536
P50	1.808	O59	−1.012
		H60	0.582

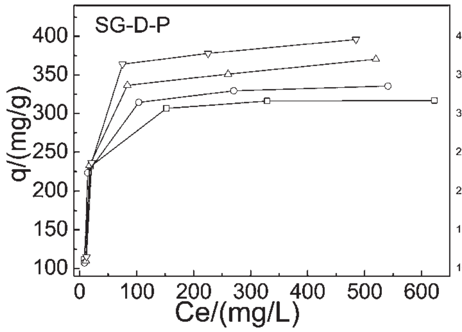

Figure 1. Isothermal adsorption of SG-D-P for Au(III) at different temperatures (□, 5 °C; ○, 15 °C; △, 25 °C; ▽, 35 °C).

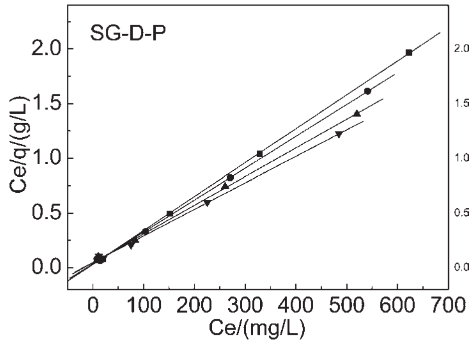

Figure 2. Langmuir isotherms of the sample SG-D-P for Au(III) at different temperatures (■, 5 °C; ●, 15 °C; ▲, 25 °C; ▼, 35 °C).

with an increase of temperature. At a certain temperature, it is clear that the adsorption capacities of Au(III) rise with an increase of the equilibrium concentration, and the maximum adsorption capacity reached 396.10 mg·g^{-1} at 35 °C in the range of the experimental concentrations. The adsorption isotherms were studied, and the data were analyzed with the Langmuir eq 2 and the Freundlich eq 3[14−16] (see Figures 2 and 3). The Langmuir model, for homogeneous adsorption systems, is represented as:

$$\frac{C_e}{q_e} = \frac{C_e}{q} + \frac{1}{qK_L} \tag{2}$$

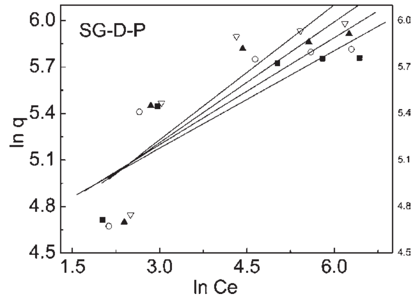

Figure 3. Freundich isotherms of the sample SG-D-P for Au(III) at different temperatures (■, 5 °C; ▽, 15 °C; ▲, 25 °C; ○, 35 °C).

Table 3. Freundlich and Langmuir Constants for Au(III) Adsorption on SG-D-P

		Langmuir			Freundlich		
	T	q	K_L		K_F		
adsorbent	°C	mg·g^{-1}	L·mg^{-1}	R^2	mg·g^{-1}	n	R^2
SG-D-P	5	322.58	0.1033	0.9998	94.151	4.7596	0.7790
	15	344.83	0.0831	0.9997	90.568	4.3365	0.7448
	25	384.62	0.0560	0.9989	83.856	3.8402	0.7306
	35	416.67	0.0503	0.9984	77.953	3.4376	0.7464

where q_e is the adsorption capacity, mg·g^{-1}; C_e is the equilibrium concentration of Au(III), mg·L^{-1}; q is the saturated adsorption capacity, mg·g^{-1}, and K_L is the Langmuir adsorption constant, L·mg^{-1}.

The Freundlich isotherm model, which describes heterogeneous adsorption systems, can be expressed as follows:

$$\ln q_e = \ln K_F + \frac{\ln C_e}{n} \tag{3}$$

where q_e is the adsorption capacity, mg·g^{-1}; C_e is the equilibrium concentration of Au(III), mg·L^{-1}; n is the Freundlich constant, and K_F is the binding energy constant reflecting the affinity of the adsorbent to the Au(III), mg·g^{-1}.

The isotherm parameters of the Langmuir and Frendlich models for the sorption of Au(III) obtained using a least-squares method are listed in Table 3. The fitting result shows that the regression coefficients R^2 obtained from the Langmuir model were very close to 1, suggesting the Langmuir model could interpret the studied adsorption procedure well. From a comparison of correlation coefficients, it can be concluded that the data were fit better by the Langmuir equation than by the Freundlich equation, indicating that the adsorption of SG-D-P for Au(III) obeyed the Langmuir adsorption isotherm. It is well-known that the Langmuir equation is applicable to homogeneous adsorption, where the adsorption of each adsorbate molecule on the surface had an equal adsorption activation energy. The fact shows that the adsorption of the hybrid adsorbent is attributed to monolayer adsorption. The obtained maximum adsorption capacity of SG-D-P for Au(III) was 322.58 mg·g^{-1} at 5 °C, 344.83 mg·g^{-1} at 15 °C, 384.62 mg·g^{-1} at 25 °C, and 416.67 mg·g^{-1} at 35 °C. Thus, this novel hybrid material has the best adsorption for Au(III). As we compared the adsorption capacity of different types of adsorbents used for Au(III) adsorption (Table 4), it was clear that the adsorption capacity of SG-D-P was relatively high when

Table 4. Adsorption Capacities of Different Adsorbents

		adsorption capacities
adsorbents	literature cited	$\mathrm{mg \cdot g^{-1}}$
GH-D-P	our work	416.67
LMCCR	17	70.34
TCF	18	54−68
alfalfa biomass	19	35.97
D1	20	89
D2	20	52
D3	20	45

Table 5. Results of Elemental Analysis of SG-D-P

		N	F^a
adsorbent	%N	$\mathrm{mmol \cdot g^{-1}}$	$\mathrm{mmol \cdot g^{-1}}$
SG-D-P	2.397	1.712	0.571

[a] $F = \%\mathrm{N} \cdot 10/14n$, where %N is the mass percentage of nitrogen in the product and n is the number of nitrogens in the ligand (for SG-D-P, $n = 3$).

Table 6. Results of Energy Spectrum Analysis of SG-D-P

						F'^a
W%	C	O	N	Si	P	$\mathrm{mmol \cdot g^{-1}}$
SG-D-P	16.47	36.16	9.20	35.02	2.39	0.67

[a] $F' = \%\mathrm{P} \cdot 10/35.5$, where %P is the mass percentage of phosphorus in the product.

compared to several other adsorbents such as L-lysine modified cross-linked chitosan resin, thiol cotton fiber, alfalfa biomass, and poly(vinylbenzylchloride-acrylonitryle-divinylbenzene) modified with tris(2-aminoethyl)amine.[17−20] The above-mentioned research results show that the novel inorganic−organic hybrid material silica gel chemically modified by diethylenetriamine bis(methylene phosphonic acid) SG-D-P is favorable and useful for the removal of precious metal ions, and the high adsorption capacity makes it a promising candidate material for Au(III) uptake.

Table 5 gives the N concentrations of the adsorbed materials determined by elemental analysis. Furthermore, it is possible to calculate the amount of attached functional groups onto the surface of silica gel (F, $\mathrm{mmol \cdot g^{-1}}$) from the percentage of nitrogen in the functionalized silica gel. The amount of F on SG-D-P was 0.571 $\mathrm{mmol \cdot g^{-1}}$. Table 6 gives the results of energy spectrum analysis of SG-D-P. As can be observed from Table 6, the mass percentage of phosphorus on GH-T-P was 2.39 %, confirming that the phosphonic acid groups were successfully introduced onto the amino-terminated chelating resin silica gel. Furthermore, it is possible to calculate the amount of attached functional groups onto the surface of the silica gel (F', $\mathrm{mmol \cdot g^{-1}}$) from the percentage of phosphorus in the functionalized silica gel. The amount of the F' of SG-D-P was 0.67 $\mathrm{mmol \cdot g^{-1}}$. Comparing the amount of the F with F', it was easy to conclude that the amount of attached functional groups from elemental analysis is consistent with that from energy spectrum analysis. Moreover, the static adsorption capacity of the resin SG-D-P for Au(III) was 1.17 $\mathrm{mmol \cdot g^{-1}}$ at 25 °C, which was close to the ligand content (about 0.62 $\mathrm{mmol \cdot g^{-1}}$). Thus, most of the functional groups of resin SG-D-P seemed to form 1:2 complexes with Au(III).

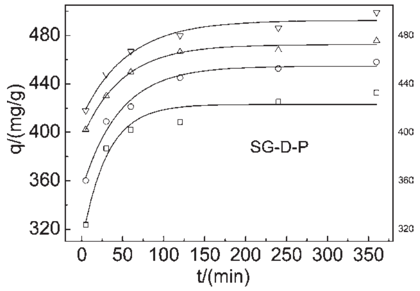

Figure 4. Adsorption kinetics of Au(III) on SG-D-P at different temperatures (□, 5 °C; ○, 15 °C; △, 25 °C; ▽, 35 °C; the initial concentration of Au(III): 2.0 $\mathrm{mmol \cdot L^{-1}}$; pH = 2.0).

Kinetic studies provide an insight into the rate as well as the mechanism of the adsorption process. To determine the uptake rate of Au(III) on the as-synthesized adsorbent and get access to the equilibrium time, studies on adsorption kinetics were carried out. The adsorption kinetics of the silica gel functionalized by diethylenetriamine bis(methylene phosphonic acid) SG-D-P for Au(III) ions at different temperatures was investigated. Figure 3 shows the adsorption kinetics of SG-D-P for Au(III) at (5 to 35) °C. As shown in Figure 4, the adsorption capacities of SG-D-P for Au(III) increased with the extension of contact time. It was obvious that, in the first 50 min, the adsorption was rapid and then slowed considerably. The reason perhaps is that in the initial fast adsorption step, Au(III) ions might enter easily the accessible pore sites and bind with the chelating ligands. While in the slow adsorption step, diffusion of some Au(III) ions into the deeper pores might be hampered. Of significant practical importance, the rapid kinetics will facilitate smaller reactor volumes, ensuring efficiency and economy. Figure 4 also displays the effect of temperature on the adsorption of Au(III) by the chelating resin SG-D-P, and it was demonstrated that temperature generally has only a slight positive effect on the adsorption capacity. From these experimental data, it was obvious that about 90 % of the equilibrium adsorption capacity could be achieved after 2 h. The adsorption equilibrium was completely achieved within 4 h under the given test conditions, and its excellent adsorption capacity for Au(III) was 499.22 $\mathrm{mg \cdot g^{-1}}$ when the initial solution concentration was 2.0 $\mathrm{mmol \cdot L^{-1}}$ at 35 °C.

The adsorption procedure of adsorbents for metal ions is generally considered to take place through two mechanisms of film diffusion and particle diffusion. The kinetics of the experimental data are often analyzed by the Boyd and Reichenberg equations[14−16] to distinguish film diffusion from particle diffusion controlled adsorption. The relevant equations are as follows:

$$F = 1 - \frac{6}{\pi^2} \sum_{n-1}^{\infty} \frac{1}{n^2} \left[\frac{-D_i t \pi^2 n^2}{r_0{}^2} \right] \tag{4}$$

$$\text{or} \quad F = 1 - \frac{6}{\pi^2} \sum_{n-1}^{\infty} \frac{1}{n^2} \exp[-n^2 Bt] \tag{5}$$

$$\text{and} \quad B = \frac{\pi^2 D_i}{r_0{}^2} = \text{time constant} \tag{6}$$

where n is an integer that defines the infinite series solution; D_i is the effective diffusion coefficient of metal ions in the adsorbent phase; r_o is the radius of the adsorbent particle, assumed to be spherical; F is the fractional attainment of equilibrium at time t and is obtained by the expression:

$$F = \frac{q_t}{q_0} \tag{7}$$

where q_t is the amount of adsorbate taken up at time t and q_o is the maximum equilibrium uptake.

Values of Bt can be obtained from corresponding values of F (eq 5), and Bt values for each F given are plotted in Figure 5; the fitting results are shown in Table 7. Plots of Bt versus time of Au(III) onto SG-D-P at (5 to 35) °C were used to distinguish between film diffusion and particle diffusion controlled adsorption. If the plots were straight lines passing through the origin, the adsorption process should be dominated by the particle diffusion mechanism; otherwise, it might be governed by the film diffusion. As seen from Figure 5, all of the lines of Bt versus time plots did not pass through the origin in the cases studied, indicating that film diffusion, not particle diffusion, dominated the adsorption processes of SG-D-P for Au(III).

Moreover, both the pseudofirst-order equation and the pseudosecond-order equation[14−16] were used to express the adsorption process of the chelating resin SG-D-P for Au(III), and they can be expressed by eqs 8 and 9, respectively:

$$\ln(q_e - q_t) = \ln q_e - k_1 t \tag{8}$$

$$\frac{t}{q_t} = \frac{1}{k_2 {q_e}^2} + \frac{t}{q_e} \tag{9}$$

where q_e is the amount of metal adsorbed at equilibrium per unit weight of adsorbent, $mg \cdot g^{-1}$, q_t is the amount of metal ion adsorbed at t time, and k_1 (min^{-1}) and k_2 ($g \cdot mg^{-1} \cdot min^{-1}$) are the rate constants of pseudofirst-order and pseudosecond-order adsorption. The experimental and calculated q_e values, k_1, k_2, and regression coefficient (R^2) values are presented in Table 8. Pseudofirst-order and pseudosecond-order kinetic plots and kinetic parameters for the sorption of Au(III) onto SG-D-P at different temperatures are shown in Figures 6 and 7, respectively. As seen from Table 8, the obtained coefficient values of the pseudosecond-order model (> 0.9997) were better than those of the pseudofirst-order model for the adsorbent (0.8161 −0.9061), suggesting that the pseudosecond-order model was more suitable to describe the adsorption kinetics of SG-D-P for Au(III). Moreover, the calculated q_e values from the pseudosecond-order model were much closer to the experimental values q_e(exp). Therefore, the adsorption kinetics could well be approximated more favorably by the pseudosecond-order kinetic model for Au(III) onto SG-D-P.

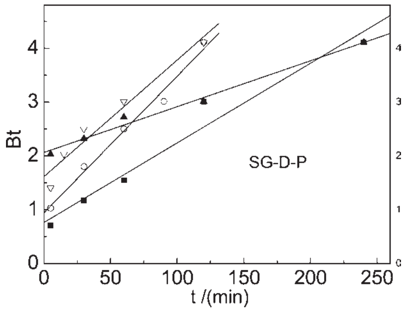

Figure 5. *Bt* versus time plots for SG-D-P at different temperatures (■, 5 °C; ○, 15 °C; ▲, 25 °C; ▽, 35 °C).

Table 7. *Bt* versus Time Linear Equations and Coefficients R^2

adsorbent	T/°C	linear equation	R^2
SG-D-P	5	$Bt = 0.0094t + 1.2781$	0.9061
	15	$Bt = 0.0125t + 1.2461$	0.9731
	25	$Bt = 0.0113t + 1.4996$	0.9827
	35	$Bt = 0.0112t + 1.4363$	0.9839

From the kinetic adsorption experiments, thermodynamic parameters, such as ΔG, ΔH, and ΔS, were obtained from the following equations:

$$K_c = \frac{C_{Ae}}{C_e} \tag{10}$$

$$\log K_c = \frac{\Delta S}{2.303R} - \frac{\Delta H}{2.303RT} \tag{11}$$

$$\Delta G = -RT \ln K_c \tag{12}$$

where C_e and C_{Ae} are the equilibrium concentration in solution ($mg \cdot L^{-1}$) and the solid phase concentration at equilibrium ($mg \cdot L^{-1}$), respectively. K_c is the partition coefficients of each temperature. R is the gas constant ($8.314 \ J \cdot mol^{-1} \cdot K^{-1}$), and T is the temperature in Kelvin. From the slope and y-intercept of the linear plot of $\ln K_c$ versus $1/T$ (shown in Figure 8), the changes of enthalpy and entropy could be obtained. The thermodynamic parameters are listed in Table 9. The negative value of ΔG at all studied temperatures ($-17.53 \ kJ \cdot mol^{-1}$ at 5 °C; $-18.79 \ kJ \cdot mol^{-1}$ at 15 °C; $-20.11 \ kJ \cdot mol^{-1}$ at 25 °C;

Table 8. Adsorption Kinetic Parameters for SG-D-P at Different Temperatures

			pseudofirst-order kinetics			pseudosecond-order kinetics		
	T	$q_{e,exp}$	k_1	$q_{e,cal}$		$k_2 \cdot 10^3$	$q_{e,cal}$	
adsorbent	°C	$mg \cdot g^{-1}$	min^{-1}	$mg \cdot g^{-1}$	${R_1}^2$	$g \cdot mg^{-1} \cdot min^{-1}$	$mg \cdot g^{-1}$	${R_2}^2$
SG-D-P	5	432.7	0.0202	148.46	0.8643	0.5238	434.78	0.9997
	15	458.2	0.0202	132.87	0.9061	0.5831	454.55	0.9999
	25	476.6	0.0224	124.89	0.8295	0.7475	476.19	0.9999
	35	498.9	0.0190	132.74	0.8161	0.5556	500.00	0.9997

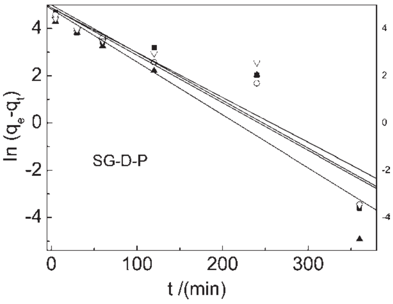

Figure 6. Pseudofirst-order kinetic plots for the sorption of Au(III) onto SG-D-P at various temperatures (■, 5 °C; ○, 15 °C; ▲, 25 °C; ▽, 35 °C).

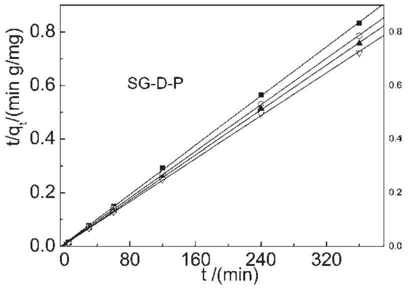

Figure 7. Pseudosecond-order kinetic plots for the adsorption of Au(III) onto SG-D-P at different temperatures (■, 5 °C; ○, 15 °C; ▲, 25 °C; ▽, 35 °C).

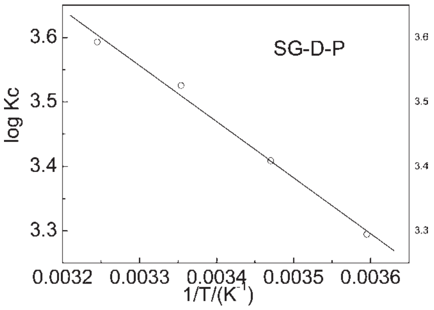

Figure 8. Enthalpy and entropy change determination for Au(III) adsorption to SG-D-P.

Table 9. Thermodynamic Parameters of SG-D-P for Au(III)

	T	ΔG	ΔH	ΔS
adsorbent	K	kJ·mol^{-1}	kJ·mol^{-1}	J·K^{-1}·mol^{-1}
SG-D-P	278	−17.53	16.59	122.86
	288	−18.79		
	298	−20.11		
	308	−21.18		

−21.18 kJ·mol^{-1} at 35 °C) for Au(III) adsorption on SG-D-P indicated that the adsorption process was spontaneous. The increase in ΔG with temperature showed that the adsorption was endothermic and more favorable at high temperature. The positive values of ΔH (16.59 kJ·mol^{-1}) indicated that Au(III) ion adsorption on SG-D-P was endothermic. This result was consistent with the above-mentioned case that the adsorption capacities of Au(III) ion increased with an increase of temperature. Since diffusion is an endothermic process, it is expected that the increased solution temperature would result in increased uptake of Au(III) ions from an aqueous solution. The positive values of ΔS (122.86 J·K^{-1}·mol^{-1}) suggest an increase in the randomness at the solid—solution interface during the adsorption process.

4. CONCLUSIONS

This preliminary study concerning the adsorption capacity of a novel hybrid material silica gel chemically modified by diethylenetriamine bis(methylene phosphonic acid) (SG-D-P) indicated great potential for rgw uptake of Au(III) from aqueous solutions. The modified organic group was theoretically studied at the B3LYP/6-31G** level and showed that the oxygen atoms in the phosphonic acid groups had more negative charges, which had advantages in chelating with metal ions in aqueous solutions. The thermodynamics and kinetics investigation of SG-D-P for the adsorption of Au(III) was studied in detail. The Langmuir and Freundlich isotherm models were applied to analyze the experimental data, and the best interpretation for the experimental data was given by the Langmuir isotherm equation. The maximum adsorption capacity for Au(III) is 416.67 mg·g^{-1} at 35 °C. Moreover, the results showed that the adsorption kinetics can be modeled by a pseudosecond-order rate equation. The thermodynamic parameters ΔG, ΔH, and ΔS were −21.18 kJ·mol^{-1}, 16.59 kJ·mol^{-1}, and 122.86 J·K^{-1}·mol^{-1}, respectively. On the basis of all results, it can be concluded that SG-D-P can effectively be used for the uptake of Au(III) ions from aqueous solutions using the adsorption method.

■ AUTHOR INFORMATION

Corresponding Author

*Tel.: + 86-535-6696162; fax: + 86-535-6697667. E-mail address: yinping426@163.com.

Funding Sources

We greatly appreciate the support provided by the Promotional Foundation for the Excellent Middle-Aged and Young Scientists of Shandong Province of China (2007BS08027), the Basic Project of Educational Bureau of Shandong Province of China (J07YA16), and the Foundation of Innovation Team Building of Ludong University (08-CXB001).

■ ACKNOWLEDGMENT

We thank Ludong University Dawning HPC Center for some theoretical calculations.

■ REFERENCES

(1) Jiang, Y.; Gao, Q.; Yu, H.; Chen, Y.; Deng, F. Intensively competitive adsorption for heavy metal ions by PAMAM-SBA-15 and EDTA-PAMAM-SBA-15 inorganic—organic hybrid materials. *Microporous Mesoporous Mater.* **2007**, *103*, 316–324.

(2) Perez-Quintanilla, D.; Hierro, I. D.; Fajardo, M.; Sierra, I. 2-Mercaptothiazoline modified mesoporous silica for mercury removal from aqueous media. *J. Hazard. Mater.* **2006**, *134*, 245–256.

(3) Liu, P.; Su, Z. Thermal stabilities of polystyrene/silica hybrid nanocomposites via microwave-assisted in situ polymerization. *Mater. Chem. Phys.* **2005**, *94*, 412–416.

(4) Jin, Y.; Li, A.; Hazelton, S. G.; Liang, S.; John, C. L.; Selid, P. D.; Pierce, D. T.; Zhao, J. X. Amorphous silica nanohybrids: Synthesis, properties and applications. *Coord. Chem. Rev.* **2009**, *253*, 2998–3014.

(5) Lesaint, C.; Lebeau, B.; Marichal, C.; Patarin, J. Synthesis of mesoporous silica materials functionalized with n-propyl groups. *Microporous Mesoporous Mater.* **2005**, *83*, 76–84.

(6) Sales, J. A. A.; Airoldi, C. Epoxide silylant agent ethylenediamine reaction product anchored on silica gel — thermodynamics of cation—nitrogen interaction at solid/liquid interface. *J. Non-Cryst. Solids* **2003**, *330*, 142–149.

(7) Roldan, P. S.; Alcântara, I. L.; Padilha, C. C. F.; Padilha, P. M. Determination of copper, iron, nickel and zinc in gasoline by FAAS after sorption and preconcentration on silica modified with 2-aminotiazole groups. *Fuel* **2005**, *84*, 305–309.

(8) Mahmoud, M. E.; El-Essawi, M. M.; Kholeif, S. A.; Fathalla, E. M. I. Aspects of surface modification, structure characterization, thermal stability and metal selectivity properties of silica gel phases-immobilized-amine derivatives. *Anal. Chim. Acta* **2004**, *525*, 123–132.

(9) Pérez-Quintanilla, D.; del Hierro, I.; Fajardo, M.; Sierra, I. Mesoporous silica functionalized with 2-mercaptopyridine: Synthesis, characterization and employment for Hg(II) adsorption. *Microporous Mesoporous Mater.* **2006**, *89*, 58–68.

(10) Anirudhan, T. S.; Radhakrishnan, P. G. Thermodynamics and kinetics of adsorption of Cu(II) from aqueous solutions onto a new cation exchanger derived from tamarind fruit shell. *J. Chem. Thermodyn.* **2008**, *40*, 702–709.

(11) Zhang, Y.; Qu, R.; Sun, C.; Chen, H.; Wang, C.; Ji, C.; Yin, P.; Sun, Y.; Zhang, H.; Niu, Y. Comparison of synthesis of chelating resin silica-gel-supported diethylenetriamine and its removal properties for transition metal ions. *J. Hazard. Mater.* **2009**, *163*, 127–135.

(12) Frisch, M. J.; Trucks, G. W.; Schlegel, H. B.; et al. *Gaussian 03*; Gaussian, Inc.: Pittsburgh, PA, 2003.

(13) Joswig, J. O.; Hazebroucq, S.; Seifert, G. Properties of the phosphonic-acid molecule and the proton transfer in the phosphonic-acid dimmer. *J. Mol. Struct.: THEOCHEM* **2007**, *816*, 119–123.

(14) Donat, R. The removal of uranium(VI) from aqueous solutions onto natural sepiolite. *J. Chem. Thermodyn.* **2009**, *41*, 829–835.

(15) Zhang, Y.; Chen, J.; Yan, X.; Feng, Q. Equilibrium and kinetics studies on adsorption of Cu(II) from aqueous solutions onto a graft copolymer of cross-linked starch/acrylonitrile (CLSAGCP). *J. Chem. Thermodyn.* **2007**, *39*, 862–865.

(16) Debnath, S.; Ghosh, U. C. Kinetics, isotherm and thermodynamics for Cr(III) and Cr(VI) adsorption from aqueous solutions by crystalline hydrous titanium oxide. *J. Chem. Thermodyn.* **2008**, *40*, 67–77.

(17) Fujiwara, K.; Ramesh, A.; Maki, T.; Hasegawa, H.; Ueda, K. Adsorption of platinum(IV), palladium(II) and gold(III) from aqueous solutions onto L-lysine modified crosslinked chitosan resin. *J. Hazard. Mater.* **2007**, *146*, 39–50.

(18) Yu, M.; Sun, D.; Tian, W.; Wang, G.; Shen, W.; Xu, N. Systematic studies on adsorption of trace elements Pt, Pd, Au, Se, Te, As, Hg, Sb on thiol cotton fiber. *Anal. Chim. Acta* **2002**, *456*, 147–155.

(19) Gamez, G.; Gardea-Torresdey, J. L.; Tiemann, K. J.; Parsons, J.; Dokken, K.; Yacaman, M. J. Recovery of gold(III) from multi-elemental solutions by alfalfa biomass. *Adv. Environ. Res.* **2003**, *7*, 563–571.

(20) Jermakowicz-Bartkowiak, D.; Kolarz, B. N.; Serwin, A. Sorption of precious metals from acid solutions by functionalised vinylbenzyl chloride-acrylonitryle-divinylbenzene copolymers bearing amino and guanidine ligands. *React. Funct. Polym.* **2005**, *65*, 135–142.